



Supplement of

Unveiling single-particle composition, size, shape, and mixing state of freshly emitted Icelandic dust via electron microscopy analysis

Agnesh Panta et al.

Correspondence to: Konrad Kandler (kandler@geo.tu-darmstadt.de)

The copyright of individual parts of the supplement might differ from the article licence.

S1 Coordinates of the sampling sites

Table S1. Coordinates of the sampling sites

ID	Coordinates
MRS	64°52'20"N 16°54'14"W
SRS	64°53'52"N 16°50'57"W
DYS (Main site)	64°54'55"N 16°46'35"W
HRS	64°57'17"N 16°40'31"W
VFS	65°01'41"N 16°26'10"W

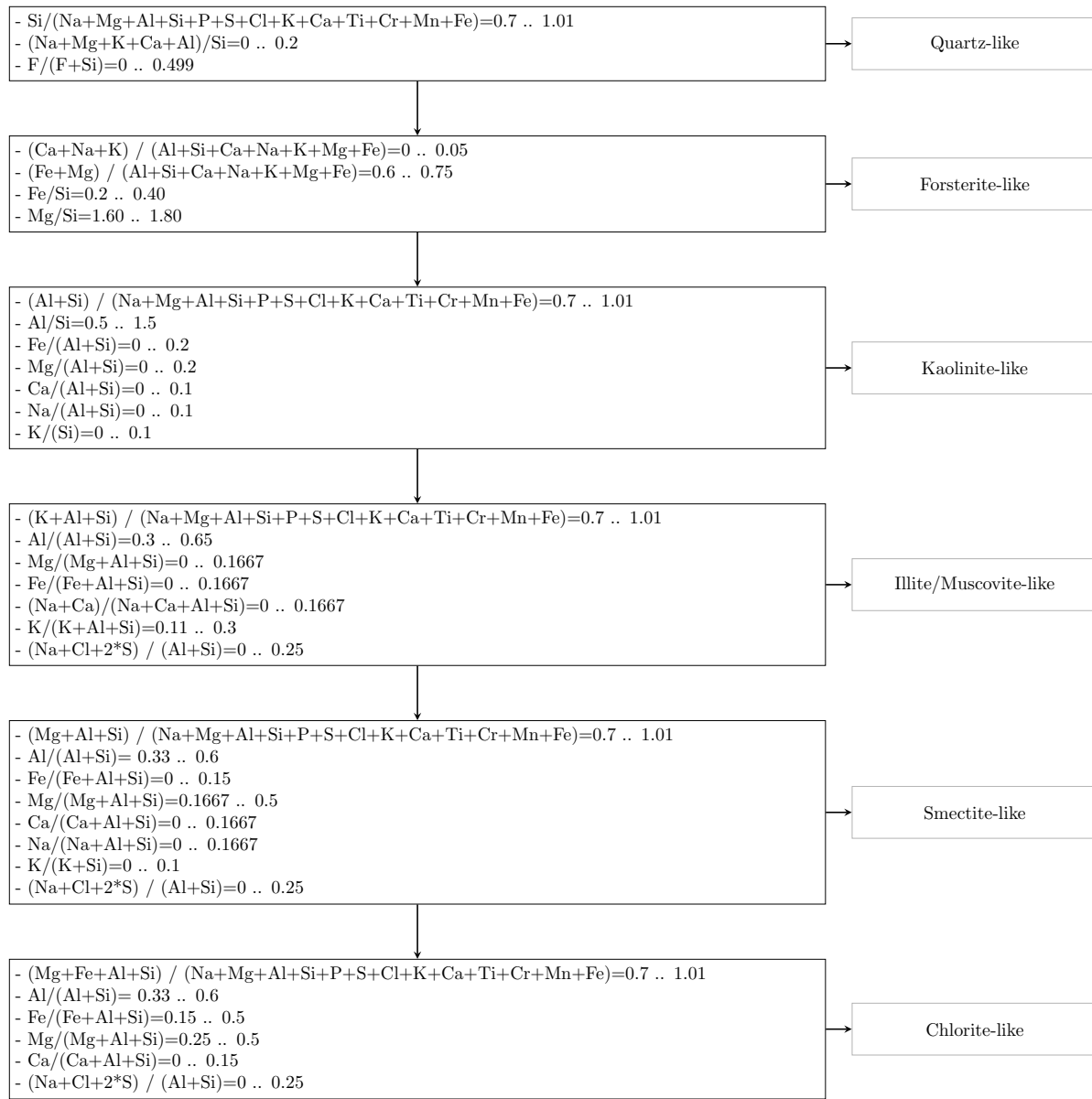
S2 Quantification of elemental composition

In our analysis, we used an acceleration voltage of 12.5 kV, which reduces the interaction volume and helps minimize the effects of particle morphology on quantification. This approach has been shown to improve accuracy, particularly for larger particles, by limiting the penetration depth of X-rays (Kandler et al., 2018). While the penetration depth of a few micrometer might pose a problem for large particles, if they exhibit a strong core-shell structure or other systematic inhomogeneities, in our case it can be expected that the effect is minor. On one hand, the beam is scanned during the analysis over all of the particle cross section, averaging out local effects. On the other hand, the mappings (section S9 below) show a homogeneous horizontal elemental distribution for the dominating particle class, which can therefore be expected to be vertically homogeneous as well (glassy matter). Also, the crystalline compounds are not expected to exhibit a strong vertical inhomogeneity; therefore in this study we can expect that the composition we measure is representative for the total particle volume.

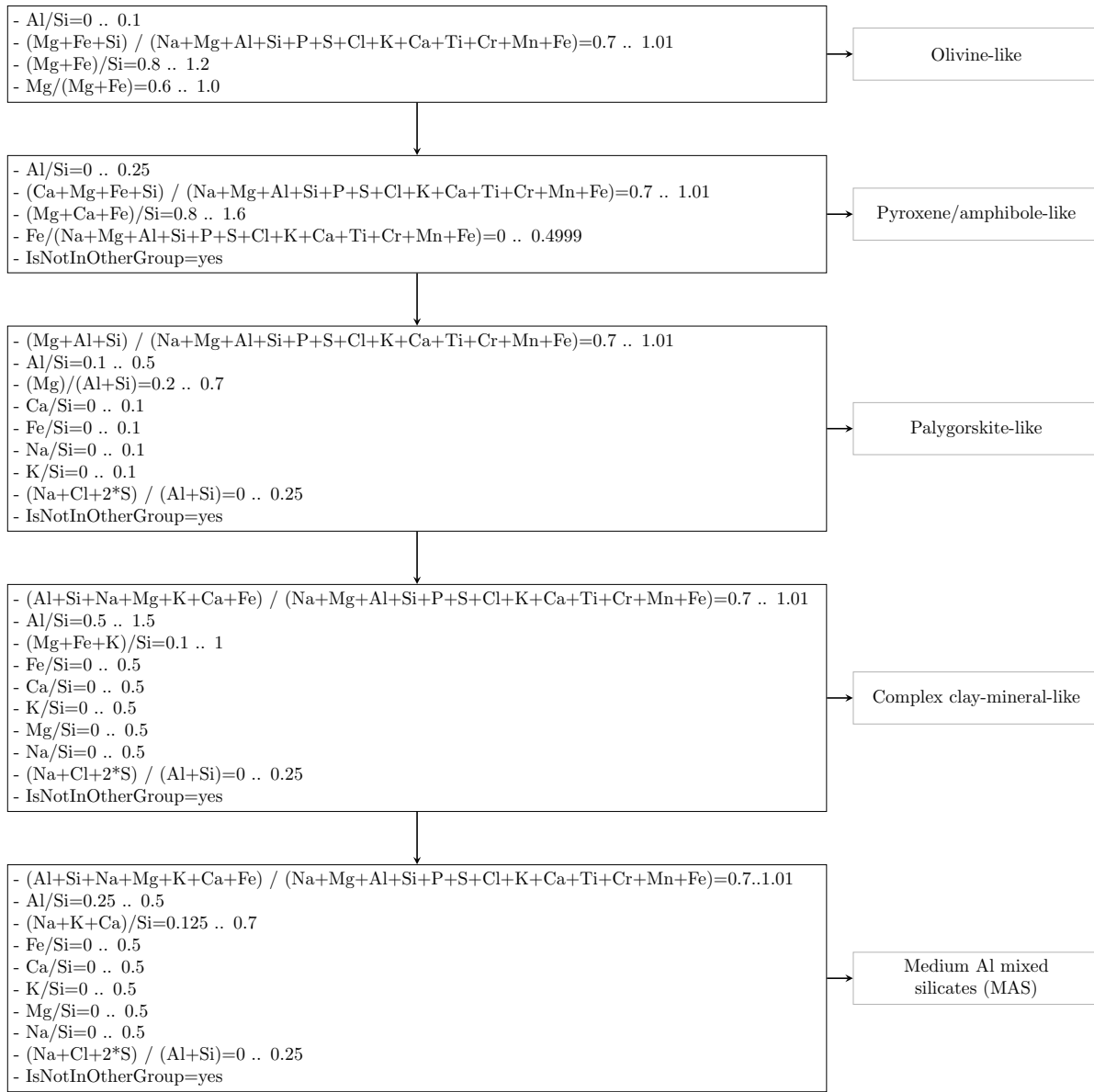
S3 SEM classification scheme

In the following, a flow chart of classification criteria is given. These criteria are displayed as range conditions for atomic percent elemental relationships, e.g. Al / Si = 0.2 .. 0.5 would indicate a criterion which matches, if the atom % ratio of Al to Si is between 0.2 and 0.5 (boundaries included). If all criteria in a box are met, a certain mineral-like group is assigned to the particle. As on one hand in the multi-dimensional element space overlaps based on simple criteria are difficult to avoid, on the other some elemental compositions for different elements are overlapping in nature as well, there are more general

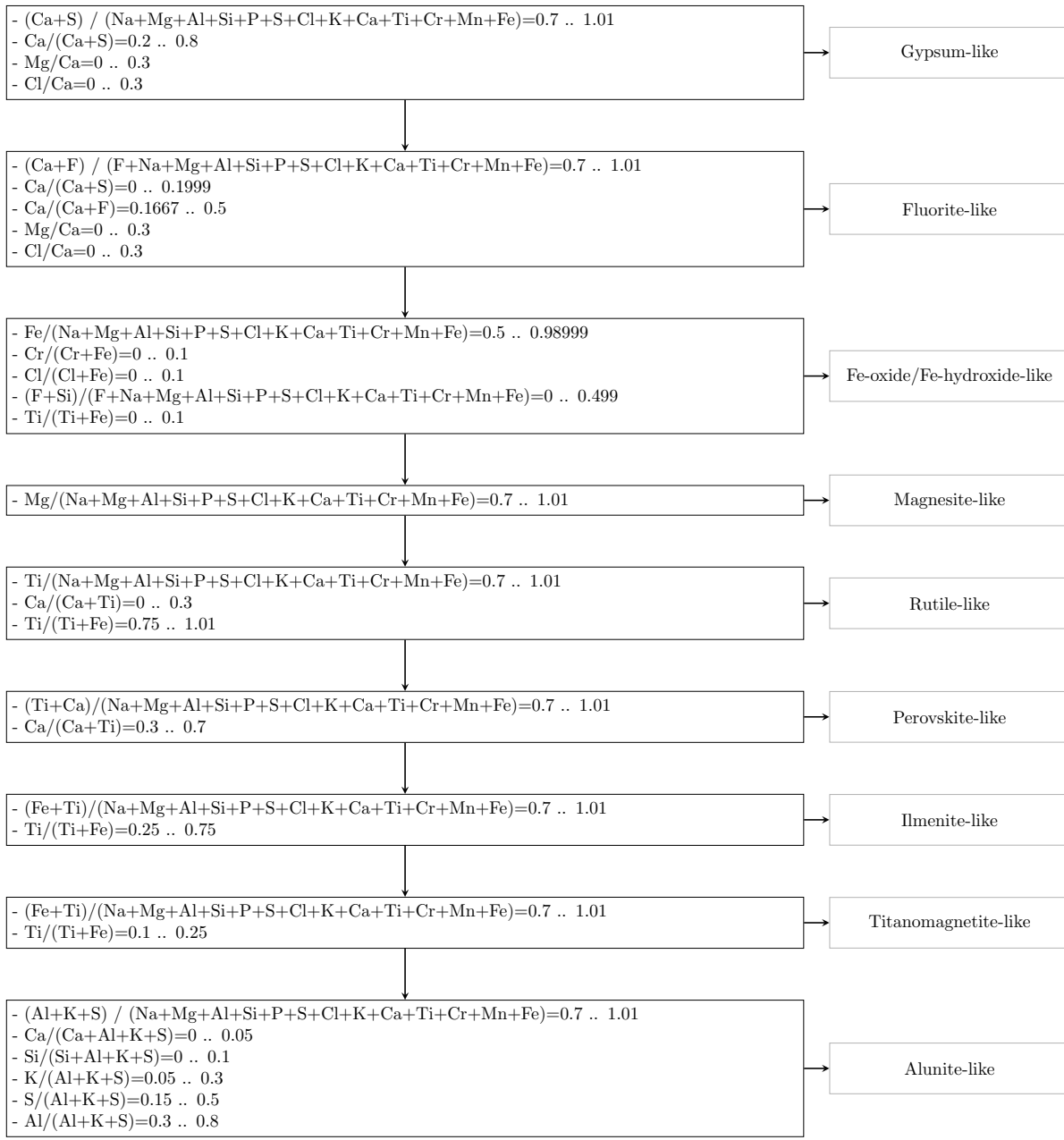
'collector groups' defined. These general (e.g., the 'Complex ...' groups) or less probable groups only trigger positively, if the particle was not assigned to another group with a more strict compositional definition before. This is indicated by the switch 'IsNotInOtherGroup=yes' in the flow chart.











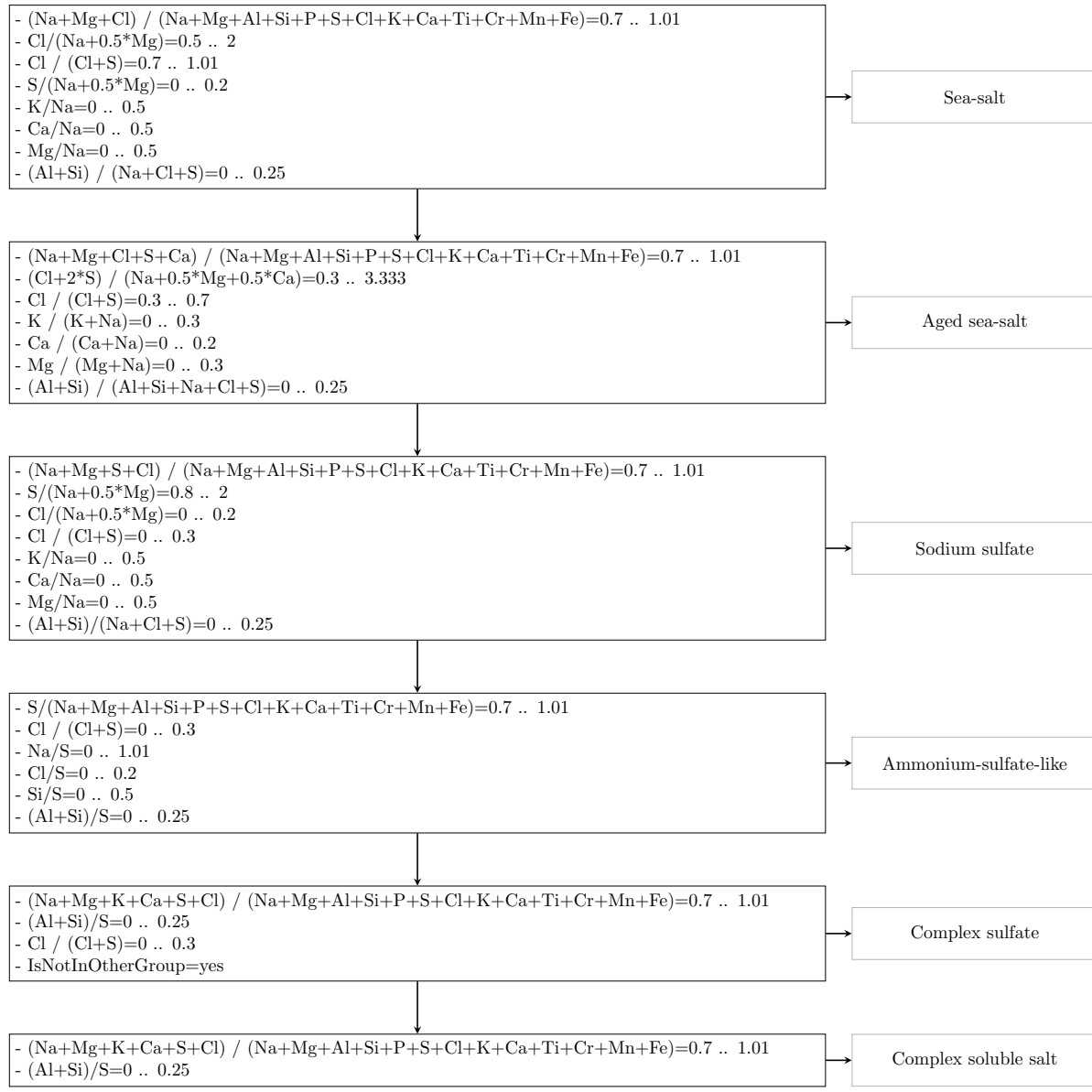




Table S2. Sampling times for flat-plate samplers at HRS

ID	Start date & time	End date & time	Exposure time (min)	ID	Start date & time	End date & time	Exposure time (min)
1	08.08.2021 19:00	10.08.2021 19:40	2920	8	23.08.2021 13:10	25.08.2021 12:15	2825
2	10.08.2021 19:40	13.08.2021 18:30	4250	9	25.08.2021 12:15	27.08.2021 14:00	2985
3	13.08.2021 18:30	15.08.2021 15:30	2700	10	27.08.2021 14:00	29.08.2021 15:30	2970
4	15.08.2021 15:35	17.08.2021 11:50	2655	11	29.08.2021 15:30	31.08.2021 19:20	3110
5	17.08.2021 11:55	19.08.2021 12:15	2900	12	31.08.2021 19:20	02.09.2021 13:55	2555
6	19.08.2021 12:20	21.08.2021 13:15	2935	13	02.09.2021 13:55	04.09.2021 09:30	2615
7	21.08.2021 13:20	23.08.2021 13:10	2870	14	04.09.2021 09:35	06.09.2021 09:30	2875

Table S3. Sampling times for flat-plate samplers at MRS

ID	Start date & time	End date & time	Exposure time (min)	ID	Start date & time	End date & time	Exposure time (min)
1	09.08.2021 09:05	11.08.2021 12:00	3055	5	17.08.2021 09:40	19.08.2021 09:00	2840
2	11.08.2021 12:00	13.08.2021 12:12	2892	6	19.08.2021 09:00	21.08.2021 09:00	2880
3	13.08.2021 12:15	15.08.2021 11:30	2835	7	21.08.2021 09:00	23.08.2021 10:00	2940
4	15.08.2021 11:30	17.08.2021 09:30	2760				

Table S4. Sampling times for flat-plate samplers at SRS

ID	Start date & time	End date & time	Exposure time (min)	ID	Start date & time	End date & time	Exposure time (min)
1	11.08.2021 12:45	13.08.2021 12:55	2890	7	23.08.2021 11:00	26.08.2021 10:00	4260
2	13.08.2021 12:58	15.08.2021 12:15	2837	8	26.08.2021 10:00	28.08.2021 10:00	2880
3	15.08.2021 12:20	17.08.2021 09:15	2695	9	28.08.2021 10:00	30.08.2021 10:20	2900
4	17.08.2021 09:20	19.08.2021 09:20	2880	10	30.08.2021 10:20	01.09.2021 11:00	2920
5	19.08.2021 09:23	21.08.2021 09:25	2882	11	01.09.2021 11:00	03.09.2021 11:00	2880
6	21.08.2021 09:28	23.08.2021 11:00	2972	12	03.09.2021 11:00	06.09.2021 11:35	4355

Table S5. Sampling times for flat-plate samplers at VFS

ID	Start date & time	End date & time	Exposure time (min)
1	12.08.2021 22:15	14.08.2021 18:10	2635
2	14.08.2021 18:15	16.08.2021 17:30	2835
3	16.08.2021 17:35	18.08.2021 18:00	2905
4	18.08.2021 18:05	20.08.2021 09:50	2385
5	20.08.2021 09:55	22.08.2021 17:40	3345
6	22.08.2021 17:40	24.08.2021 11:10	2490

ID	Start date & time	End date & time	Exposure time (min)
7	24.08.2021 11:15	27.08.2021 09:00	4185
8	27.08.2021 09:05	29.08.2021 09:30	2905
9	29.08.2021 09:30	31.08.2021 10:25	2935
10	31.08.2021 10:25	02.09.2021 10:15	2870
11	02.09.2021 10:15	04.09.2021 10:30	2895

S4 Relative Abundances of Various Types of Particles

Table S6. Size resolved volume fraction (%) of particles in each particle class (number fraction in parentheses).

Particle type	Size class in μm						
	0.1-1	1-2	2-4	4-8	8-16	16-32	32-64
Fe-oxide/Fe-hydroxide-like	3.42 (3.47)	1.23 (1.76)	0.46 (0.48)	0.19 (0.21)	0.13 (0.15)	0.06 (0.11)	
Titanomagnetite-like	1.74 (1.76)	0.79 (0.87)	0.42 (0.47)	0.11 (0.15)	0.03 (0.05)		
Quartz-like	2.01 (1.85)	0.92 (1.25)	0.32 (0.35)	0.13 (0.15)	0.11 (0.12)	0.06 (0.09)	
Complex quartz-like	1.48 (1.45)	1.82 (1.79)	2.06 (2.06)	1.85 (1.87)	1.57 (1.55)	0.99 (0.99)	0.75 (1.01)
Pyroxene/amphibole-like	4.95 (4.88)	5.79 (5.91)	4.81 (5.05)	3.64 (3.81)	2.42 (2.72)	0.84 (0.92)	0.08 (0.17)
Albite-like	0.14 (0.15)	0.22 (0.22)	0.16 (0.17)	0.15 (0.15)	0.09 (0.12)	0.03 (0.05)	0.20 (0.17)
Interm.-Plag.-like	5.83 (5.55)	7.81 (8.09)	6.88 (7.19)	4.93 (5.29)	3.57 (3.84)	1.82 (2.00)	0.95 (1.35)
Anorthite-like	1.85 (1.76)	2.84 (2.80)	2.13 (2.26)	1.92 (1.97)	1.49 (1.57)	0.98 (1.03)	1.34 (1.01)
Complex silicate (moderat Al-low alkali)	6.79 (7.12)	2.88 (3.66)	1.87 (2.00)	0.86 (1.03)	0.46 (0.49)	0.70 (0.54)	0.52 (0.51)
Complex silicate (high Al)	1.23 (1.28)	0.84 (0.98)	0.30 (0.35)	0.24 (0.25)	0.11 (0.12)	0.14 (0.13)	
Al-rich clay mineral	1.01 (0.65)	1.01 (0.42)	1.41 (0.18)	1.08 (0.06)	1.03 (0.03)	0.90 (0.04)	
Other silicate	13.19 (13.62)	7.20 (8.34)	3.34 (3.71)	2.06 (2.18)	1.61 (1.65)	1.42 (1.48)	1.39 (1.69)
Ca-rich silicate/Ca-Si-mixture	1.45 (1.53)	1.59 (1.45)	1.26 (1.24)	1.40 (1.39)	1.05 (1.14)	0.61 (0.65)	0.98 (0.68)
Medium Al mixed silicates	35.50 (34.15)	56.72 (52.74)	68.80 (67.42)	79.26 (77.36)	86.87 (85.78)	91.99 (91.72)	93.68 (93.24)
Olivine-like	0.37 (0.34)	0.24 (0.23)	0.09 (0.11)	0.07 (0.08)	0.03 (0.05)		
Calcite-like	1.41 (1.60)	0.59 (0.76)	0.22 (0.26)	0.06 (0.07)	0.02 (0.02)		
Gypsum-like	1.80 (1.85)	0.78 (0.87)	0.10 (0.13)	0.04 (0.05)	0.02 (0.02)	0.01 (0.02)	
Ammonium-sulfate-like	5.36 (4.96)	3.80 (3.43)	5.45 (5.30)	2.19 (2.87)	0.20 (0.33)	0.02 (0.04)	
Complex sulfate	1.64 (1.74)	0.42 (0.59)	0.15 (0.14)	0.20 (0.24)	0.01 (0.03)		
Sulfate/silicate mixture	0.80 (0.88)	0.37 (0.41)	0.11 (0.13)	0.10 (0.11)	0.01 (0.03)	0.01 (0.02)	
Other	8.48 (9.41)	2.79 (3.43)	0.88 (0.99)	0.58 (0.72)	0.19 (0.21)	0.28 (0.18)	0.11 (0.17)

S5 Temporal evolution

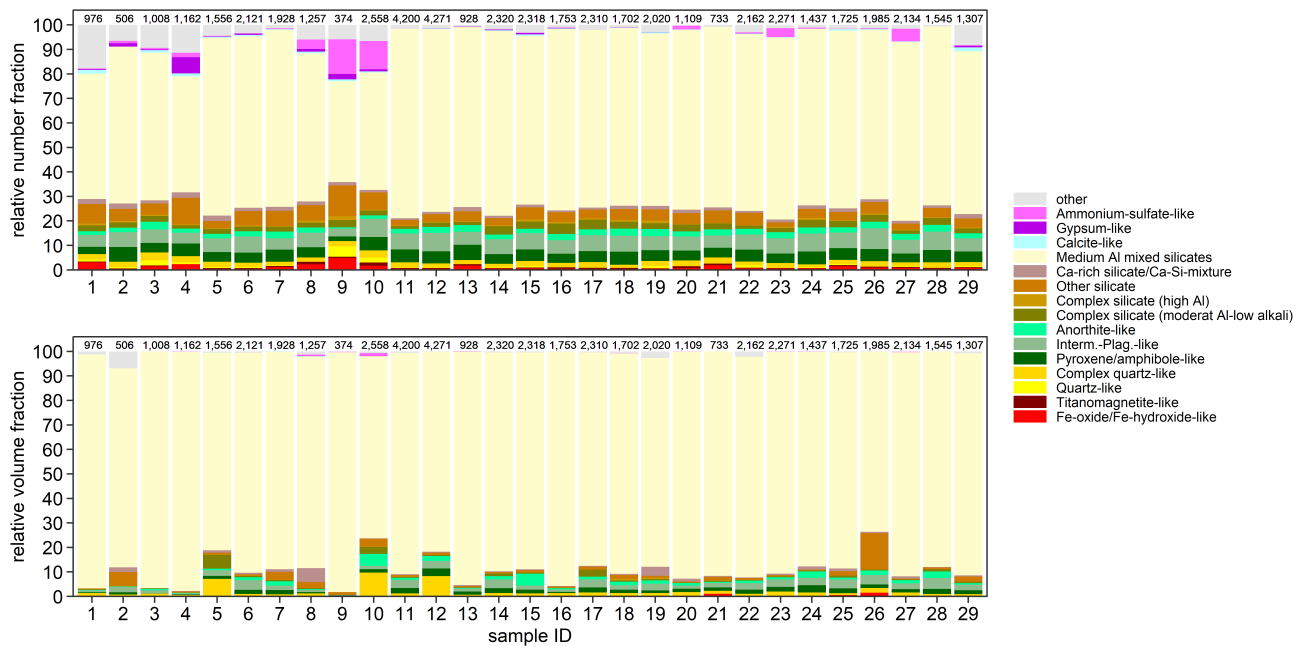


Figure S1. Chemical composition (relative number and volume abundance) of different particle groups of aerosol collected in August and September 2021 at Dyngjusandur by deposition plate sampler. The numbers on top represent total particle analysed.

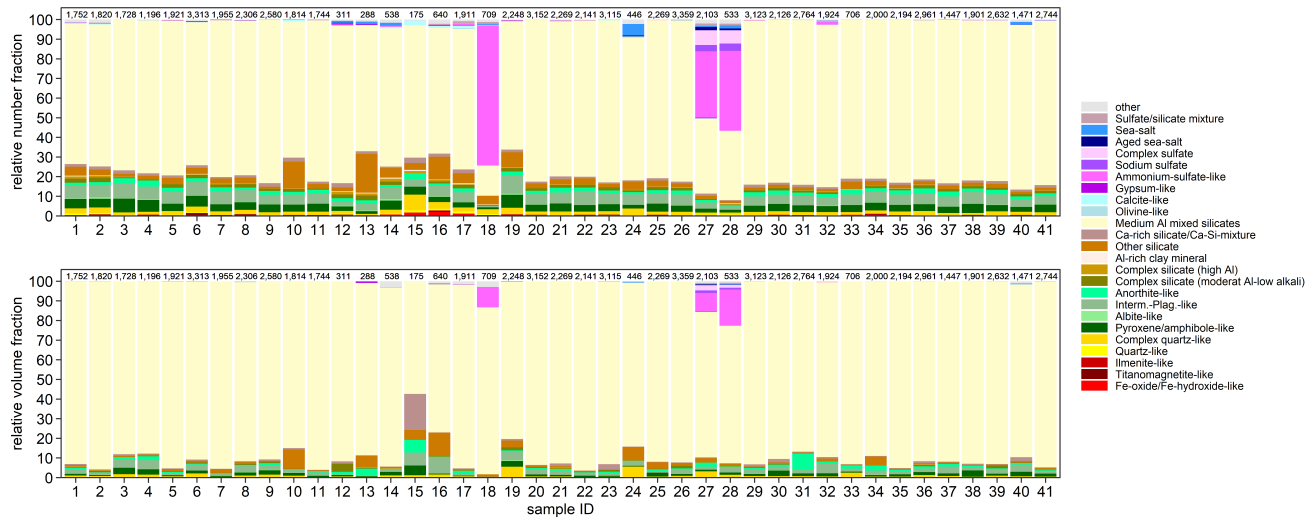


Figure S2. Chemical composition (relative number and volume abundance) of different particle groups of aerosol collected in August and September 2021 at Dyngjusandur by free-wing impactor. The numbers on top represent total particle analysed.

S6 Aspect ratio frequency distribution for select particle class

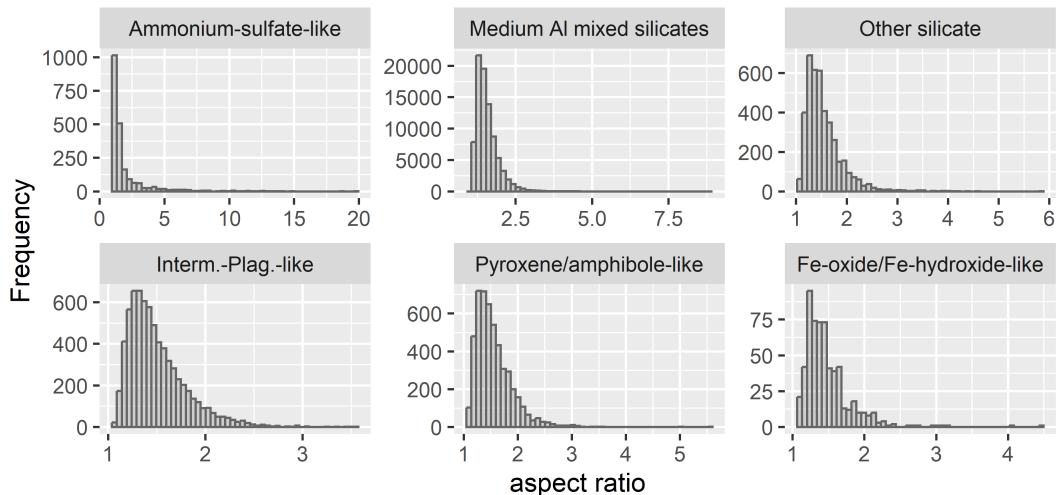


Figure S3. A selected particle group aspect ratios of the Icelandic dust at Dyngjusandur. Full range was 1.03 to 19.65 (1.0 being spherical). The majority of particles had an aspect ratio < 3.

S7 Overview of collected particles

The image highlights the diversity of the dust grains in terms of size and surface structure.

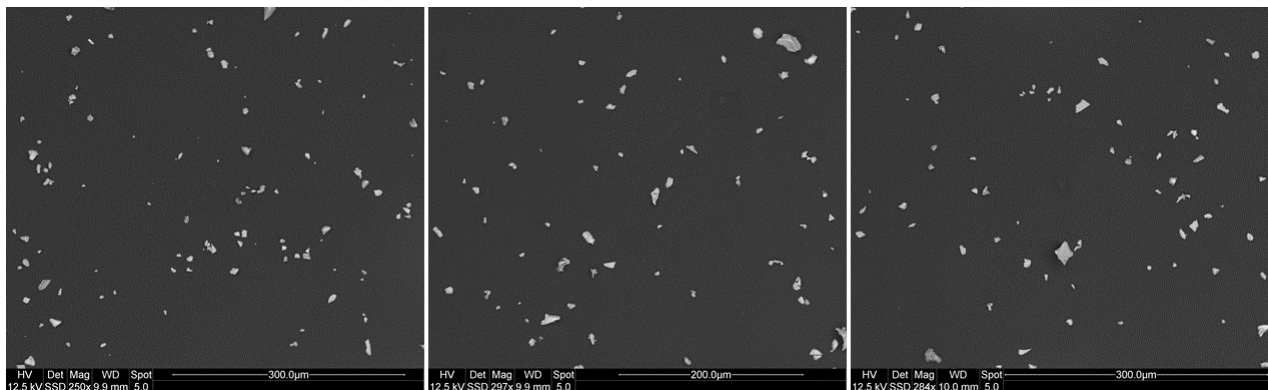


Figure S4. Examples of low-magnification backscatter electron micrographs of dust collected by the flat-plate deposition sampler in Dynjusandur, Iceland. Most dust particles exhibit non-spherical, irregular features.

S8 SEM image of coarse and super-coarse MAS particle

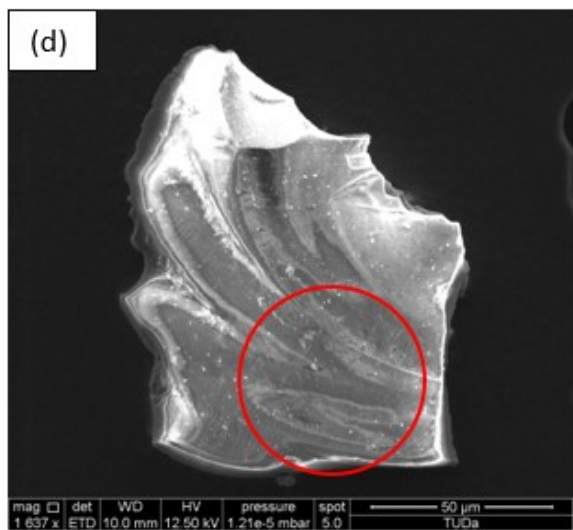
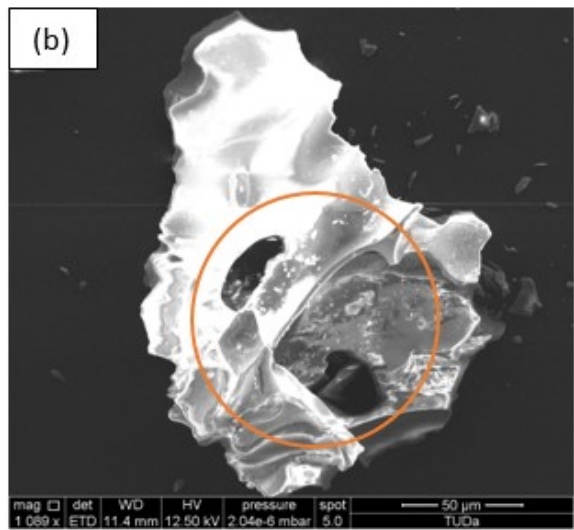
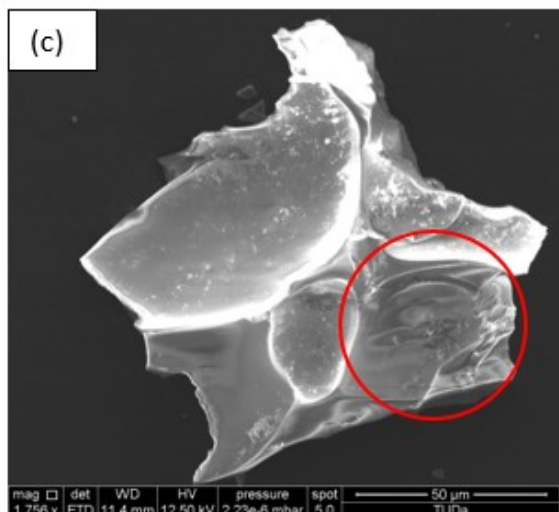
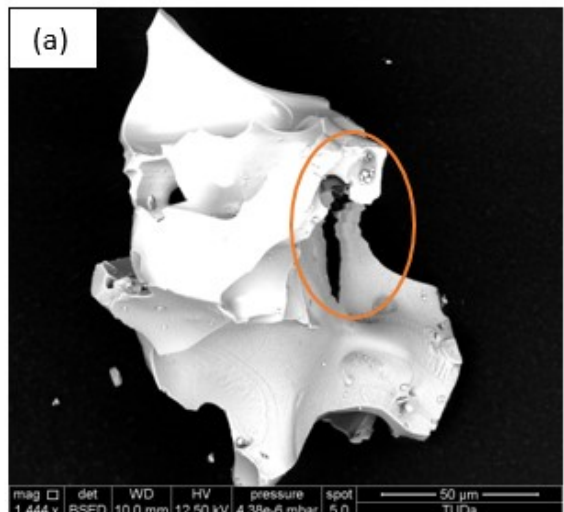


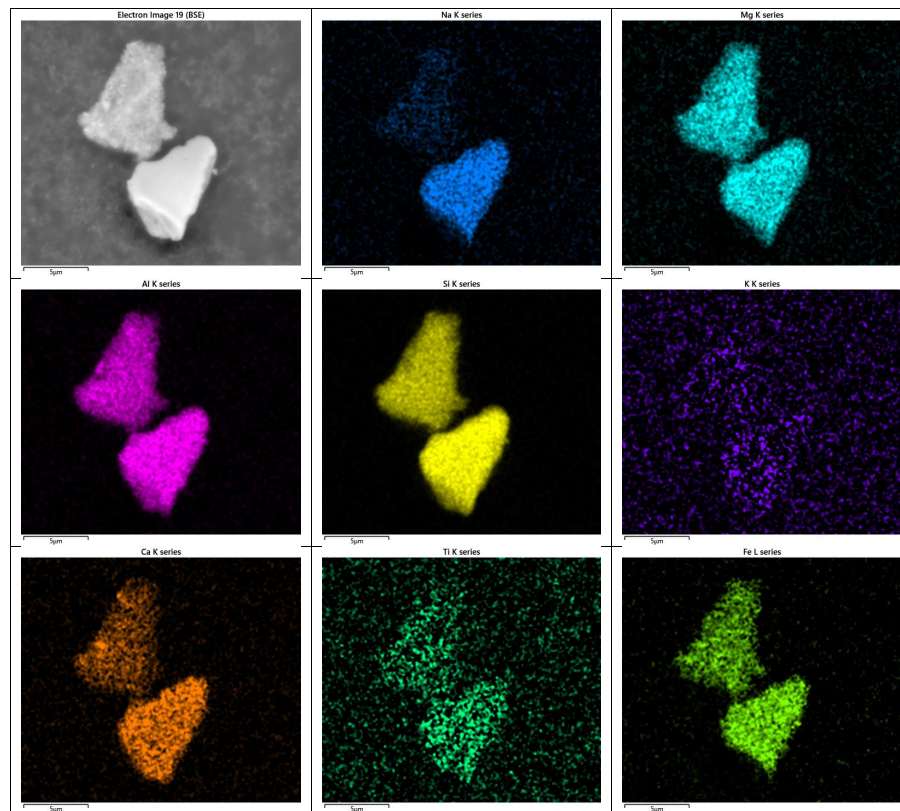
Figure S5. Morphological features of some typical coarse and super-coarse MAS particle collected at Dyngjusandur. (a) and (b) highlights the presence of voids as well as fine particles and (c) and (d) shows typical river line fractures.

S9 Elemental mapping of MAS particles

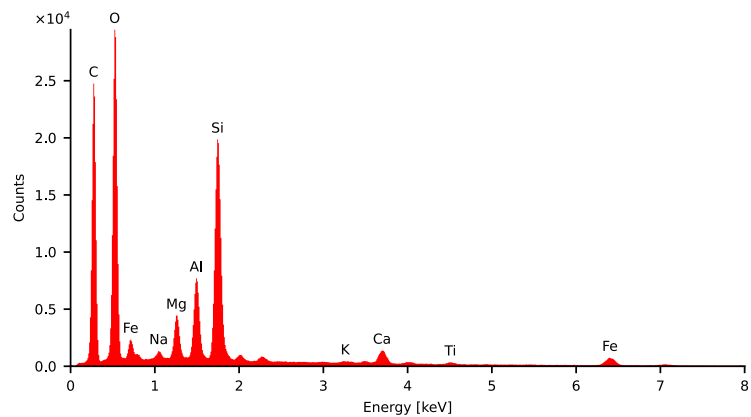
Backscatter electron image and characteristic peak net intensity maps for glassy solid and pumice-like silicate particles. The elemental maps are normalized to the highest intensity each. In addition, a sum spectrum for the particle – or the regions denominated at the spectrum – is given. Note that the lower X-ray energy maps show shading effects due do particle-internal absorption.

Elemental maps of Sodium (Na), Magnesium (Mg), Aluminum (Al), Silicon (Si), Potassium (K), Calcium (Ca), Titanium (Ti), and Iron (Fe) are shown below, labeled from (a) to (m). Increased brightness indicates higher concentrations of the element. The white circles in images (d) and (g) highlight the Fe-rich inclusions, (c) shows a Fe-Ti grain, and (k) shows an Mg-rich grain.

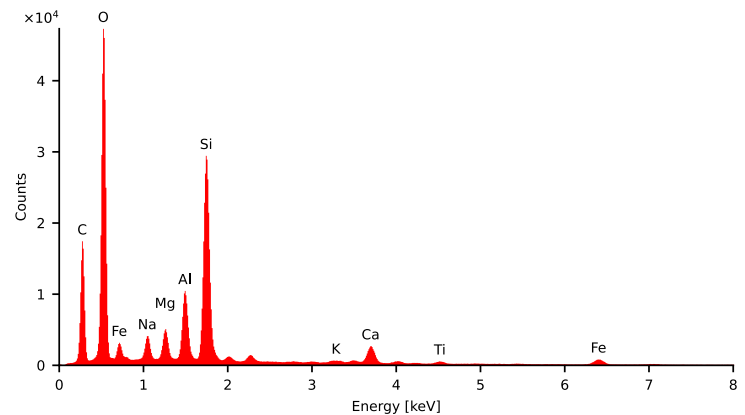
a)



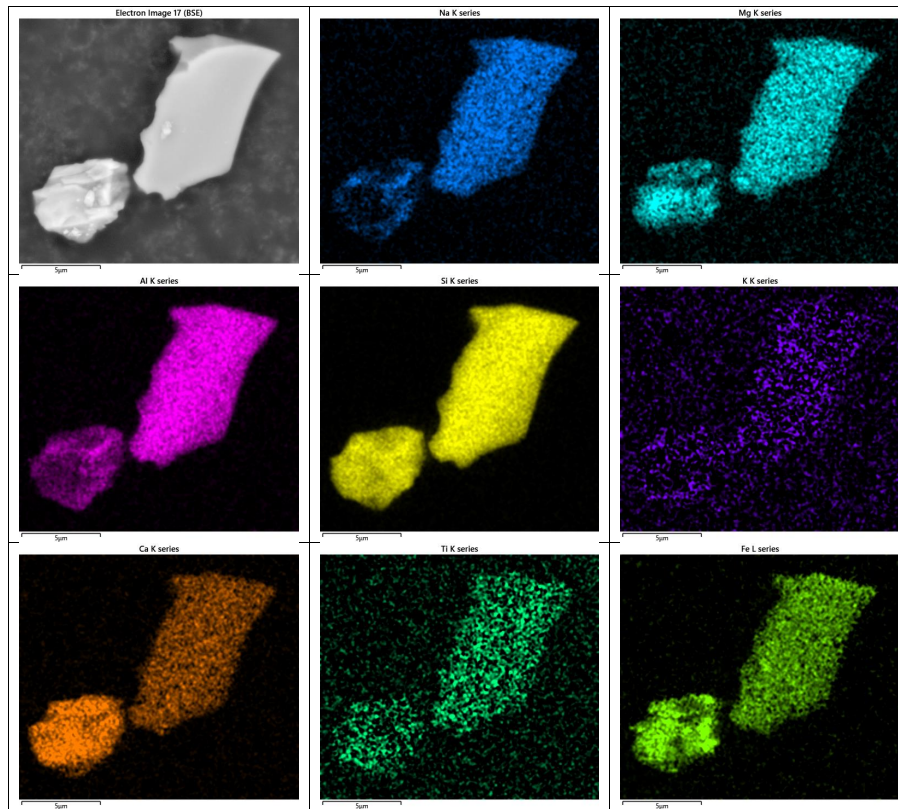
Upper particle



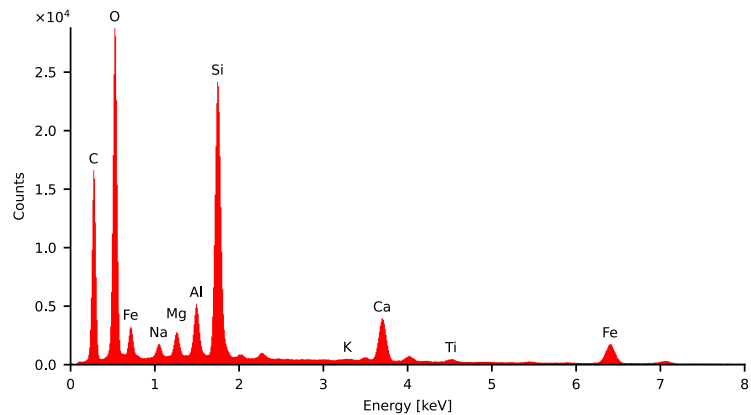
Lower particle



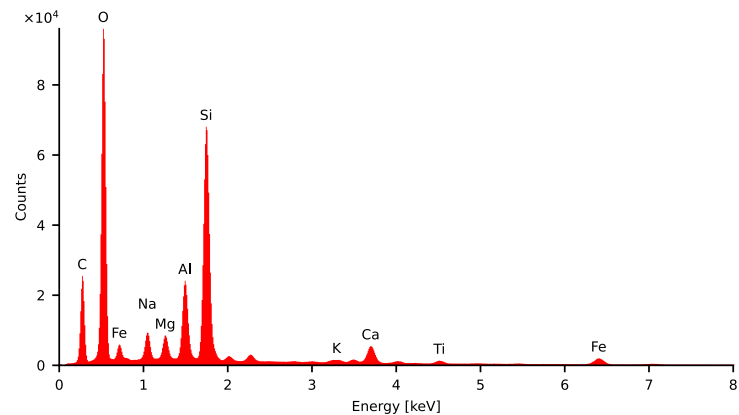
b)



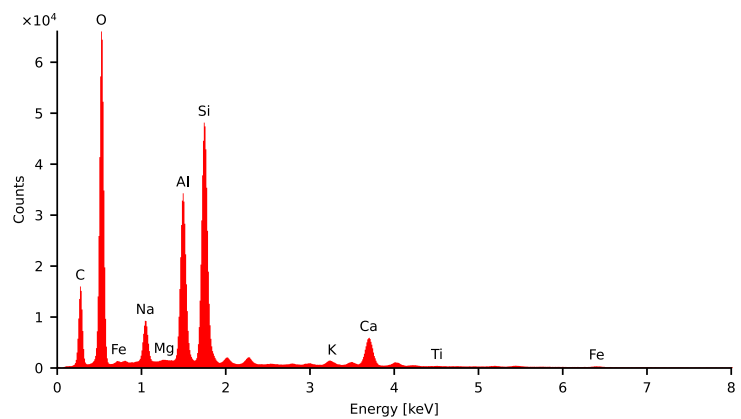
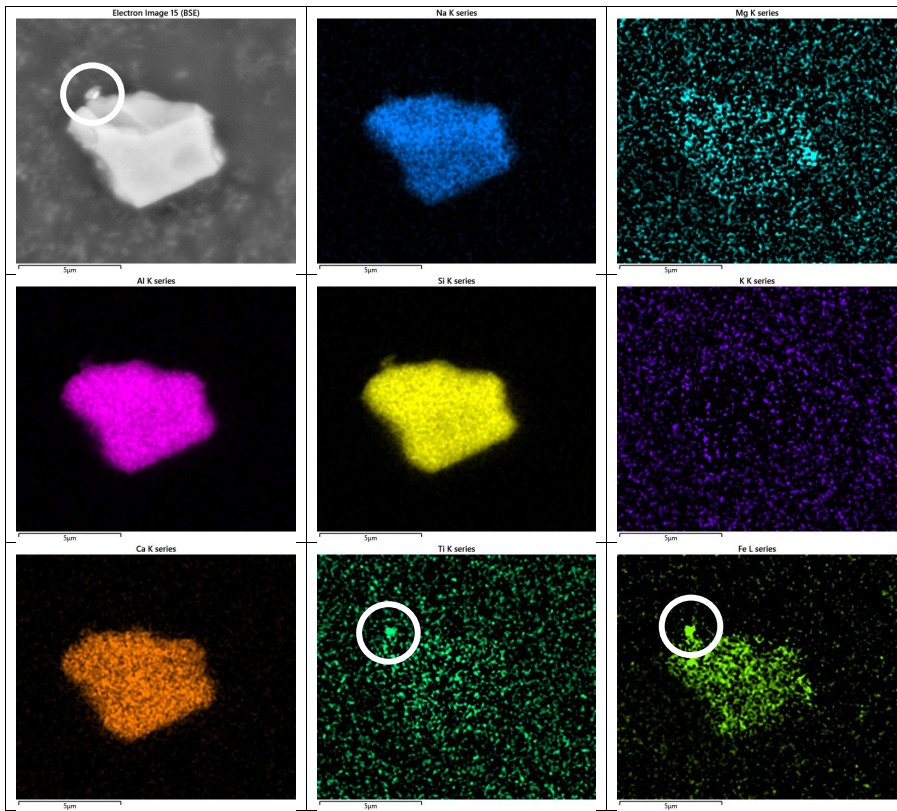
Left particle



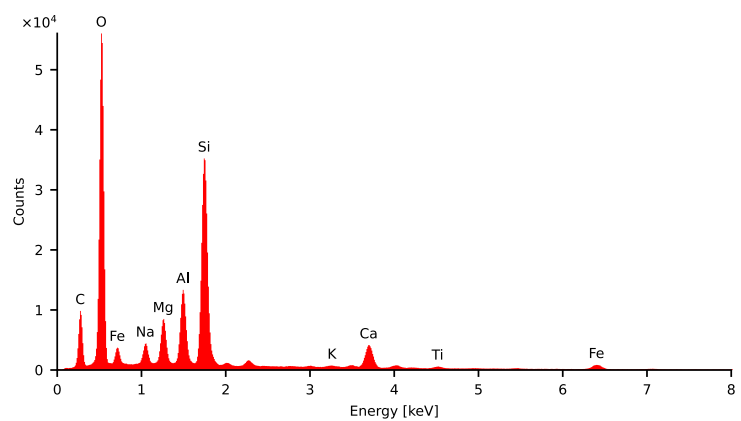
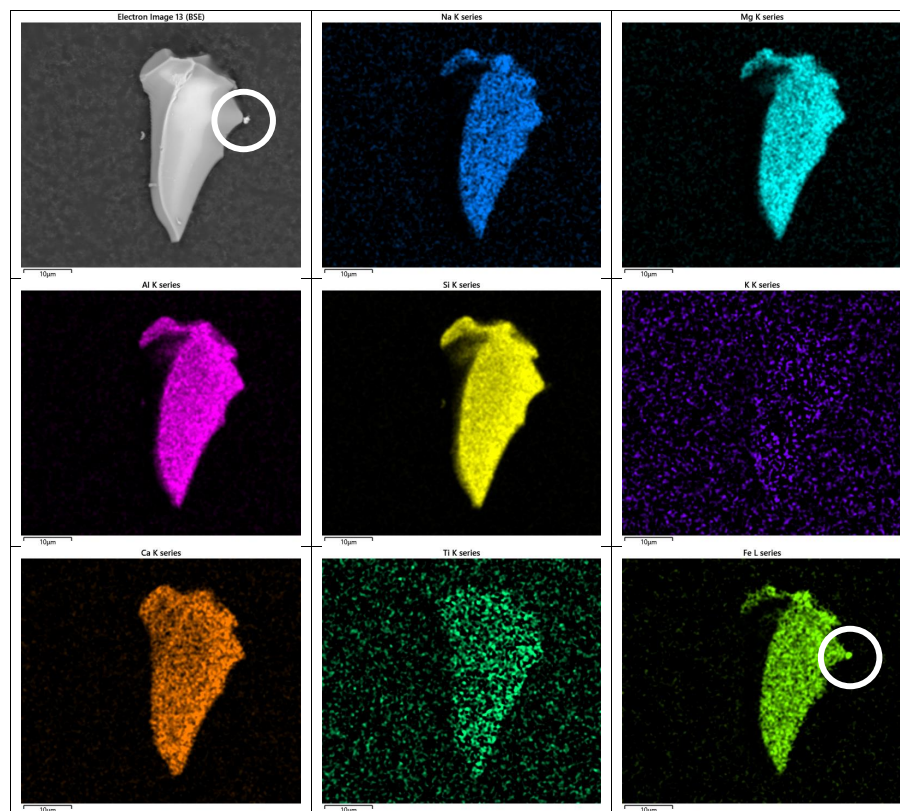
Right particle



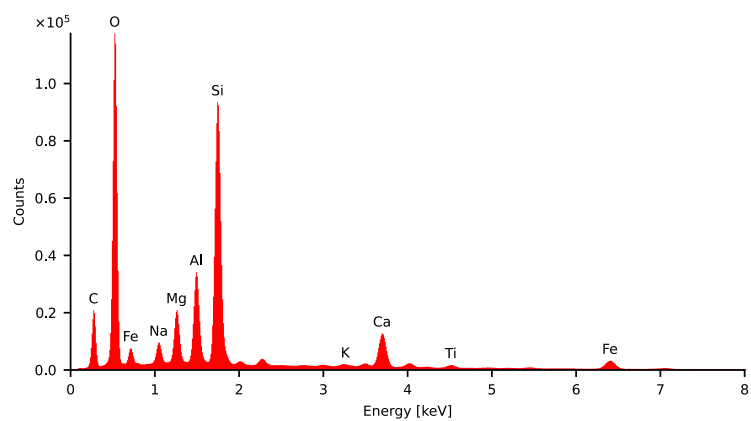
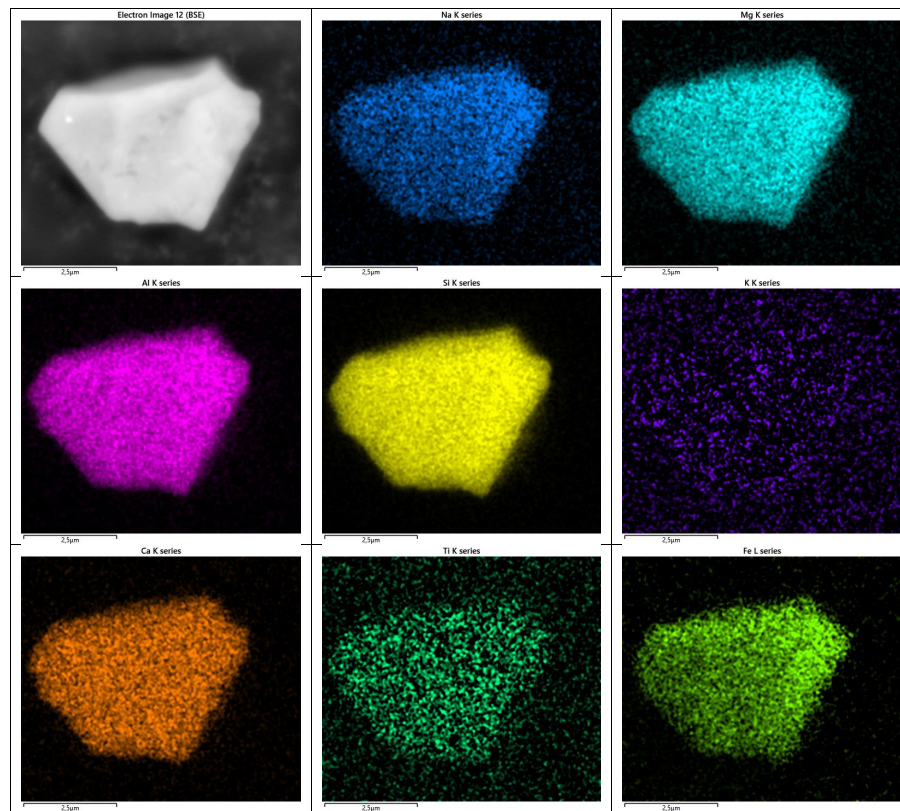
c)



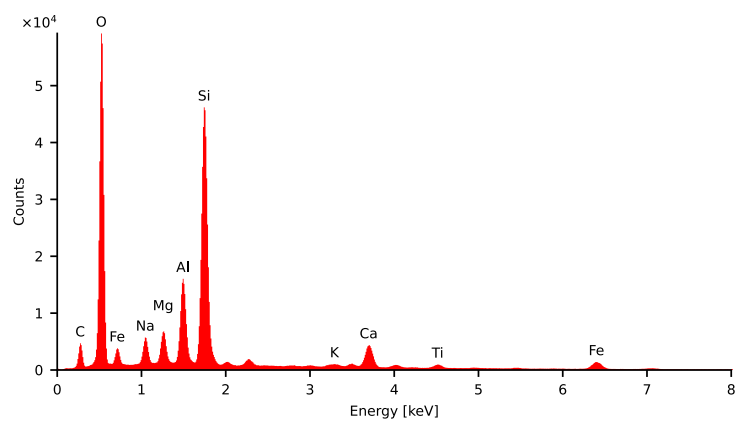
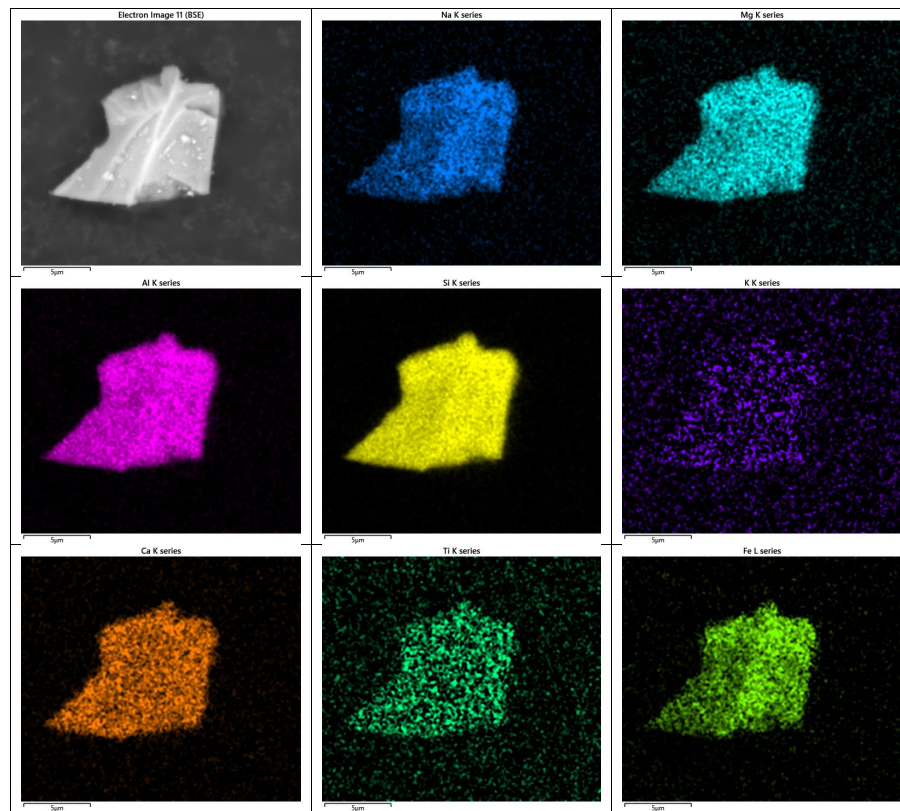
d)



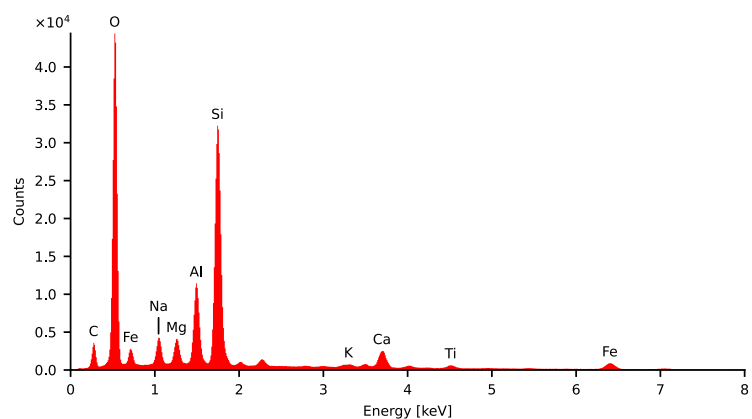
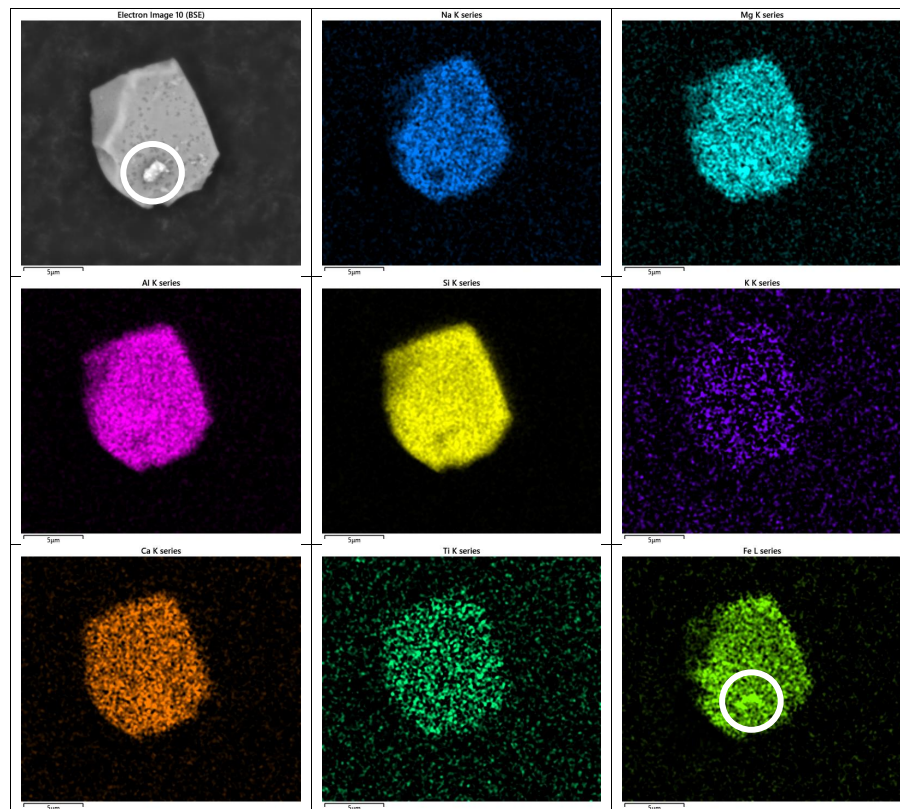
e)



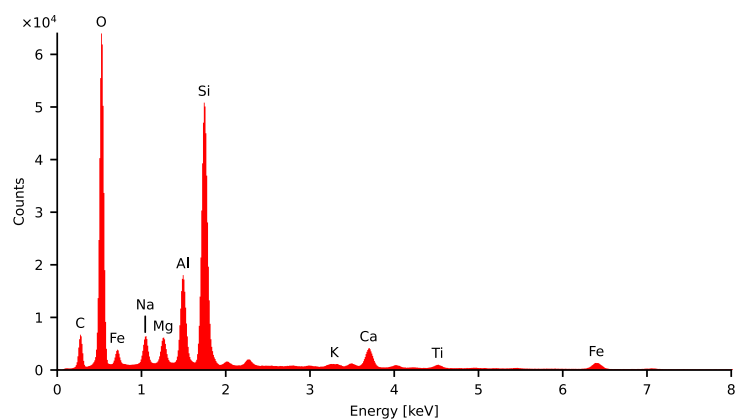
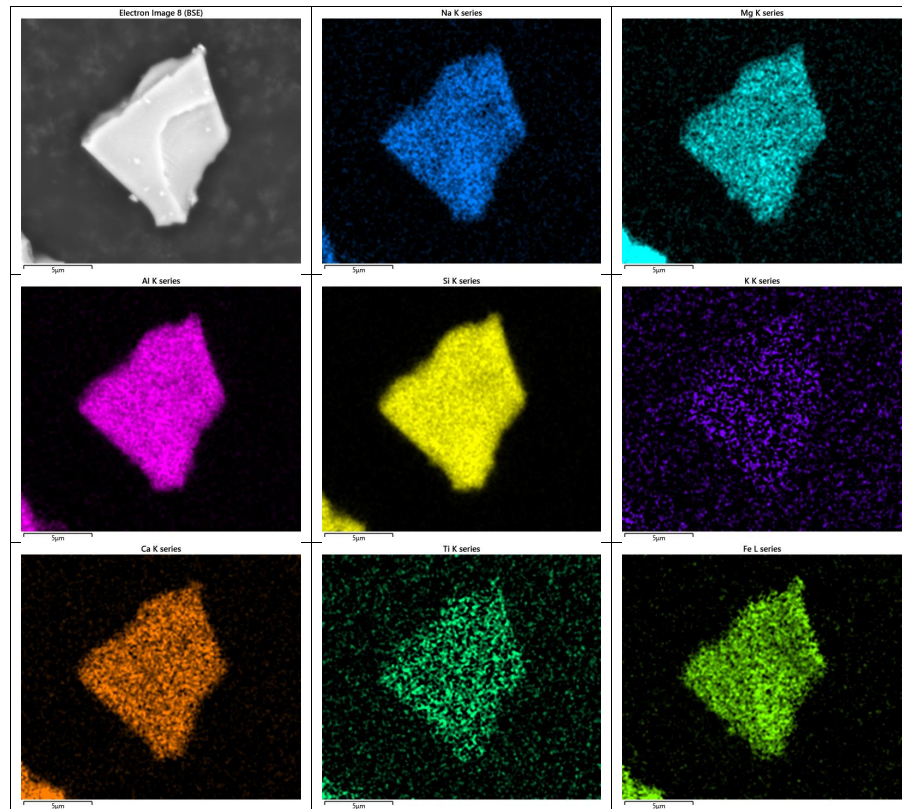
f)



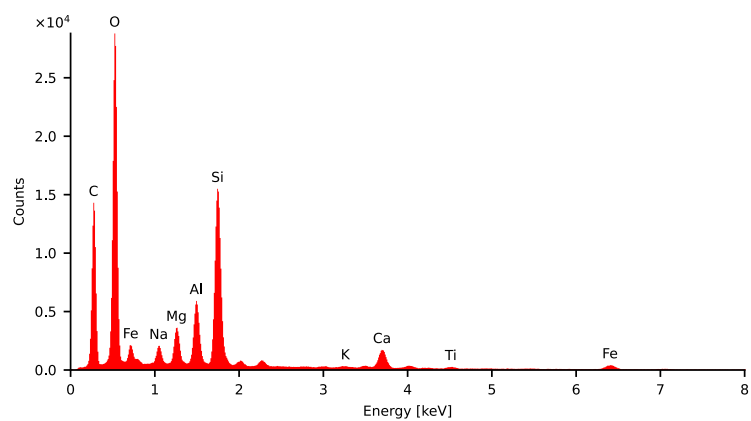
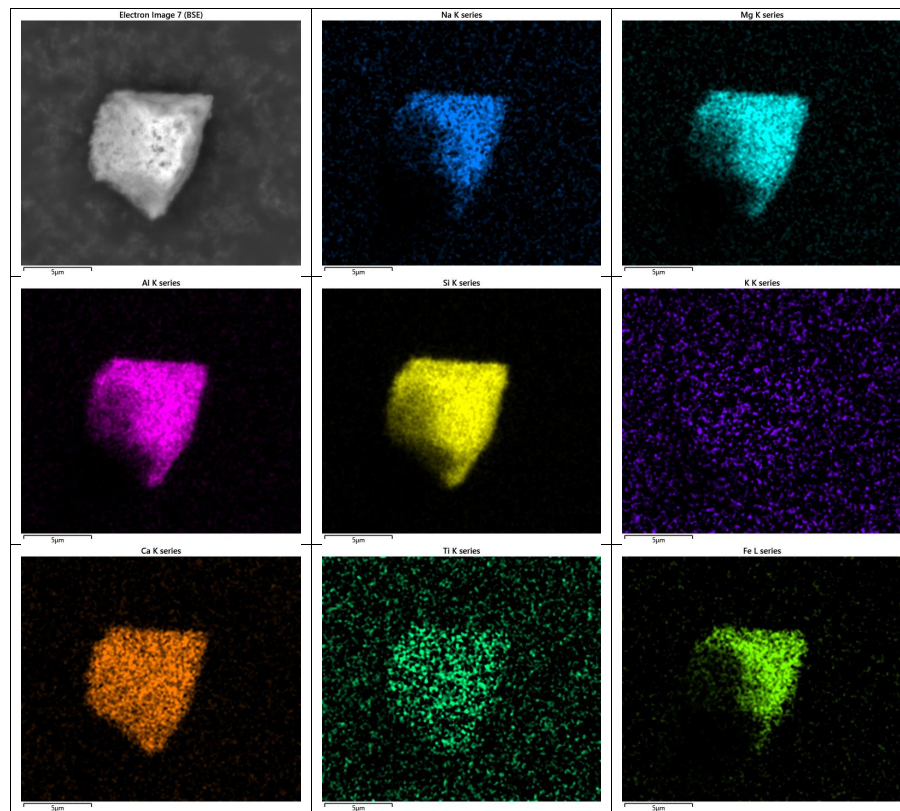
g)



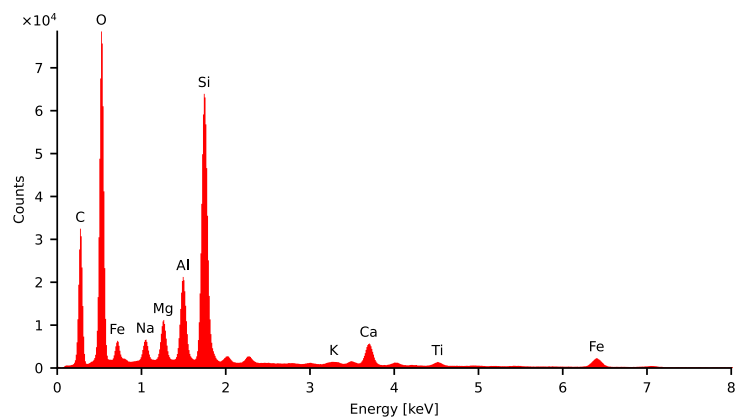
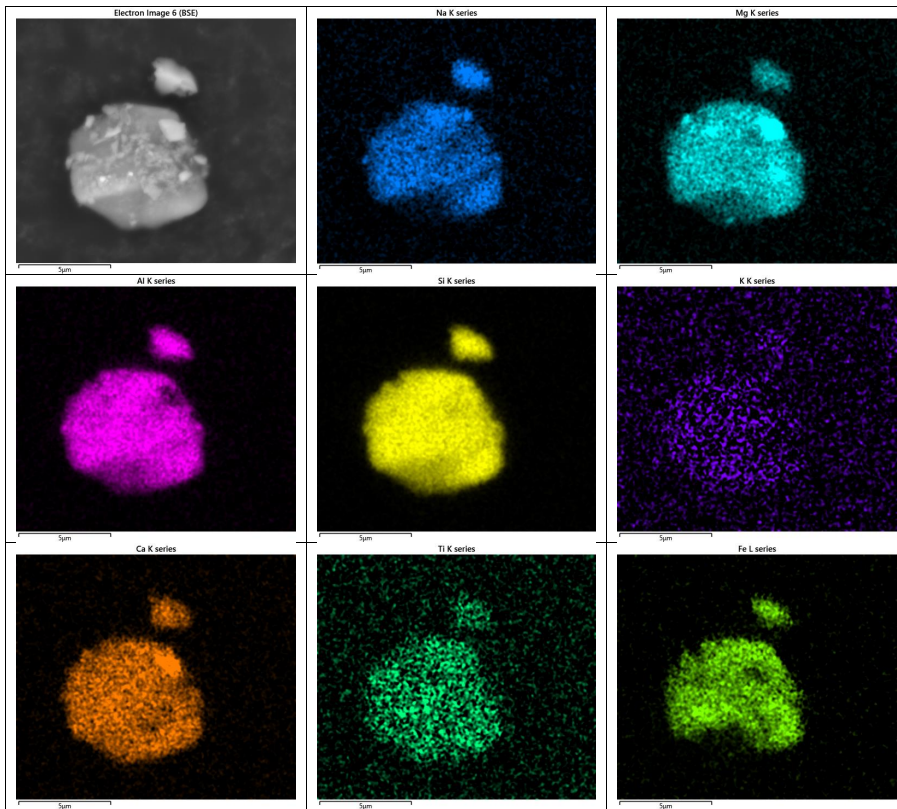
h)



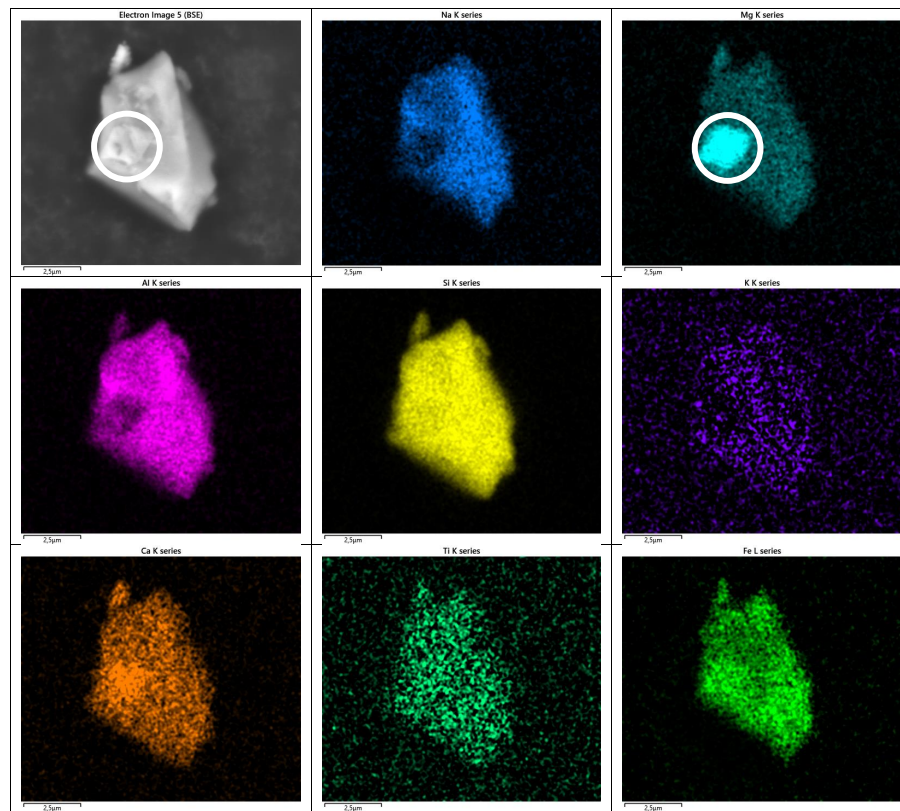
i)



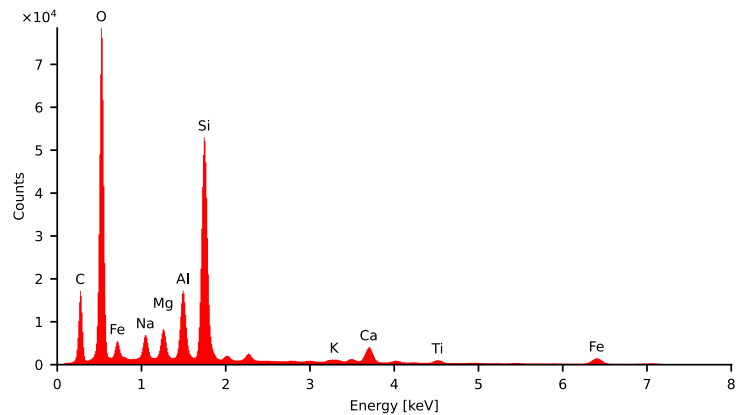
j)



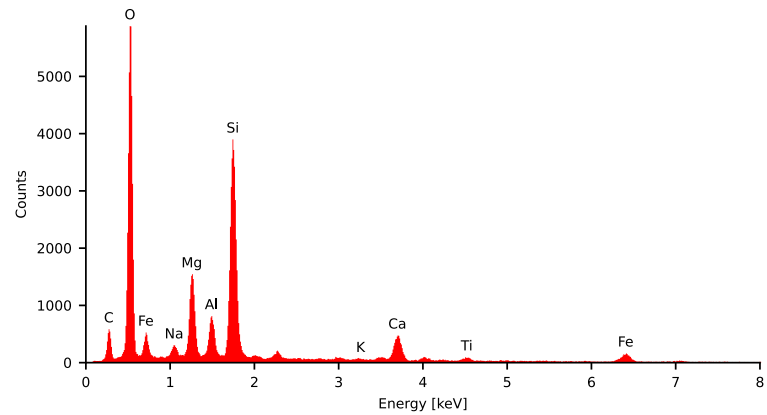
k)



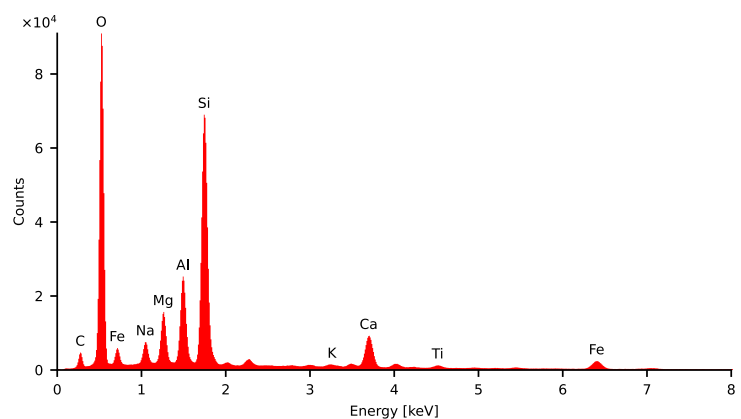
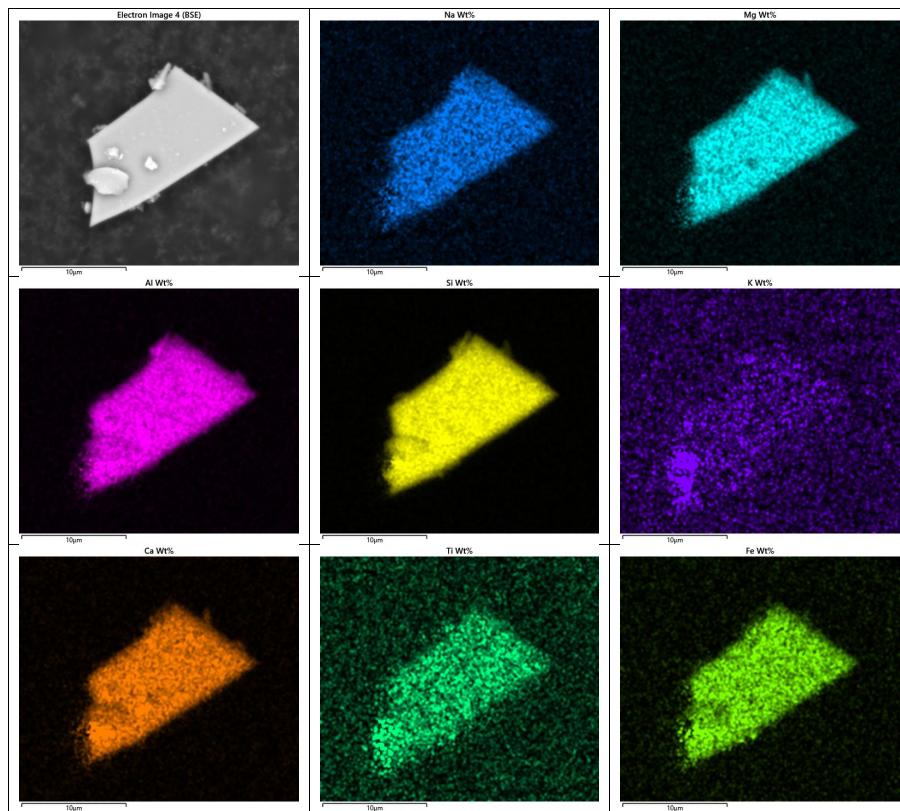
Large particle



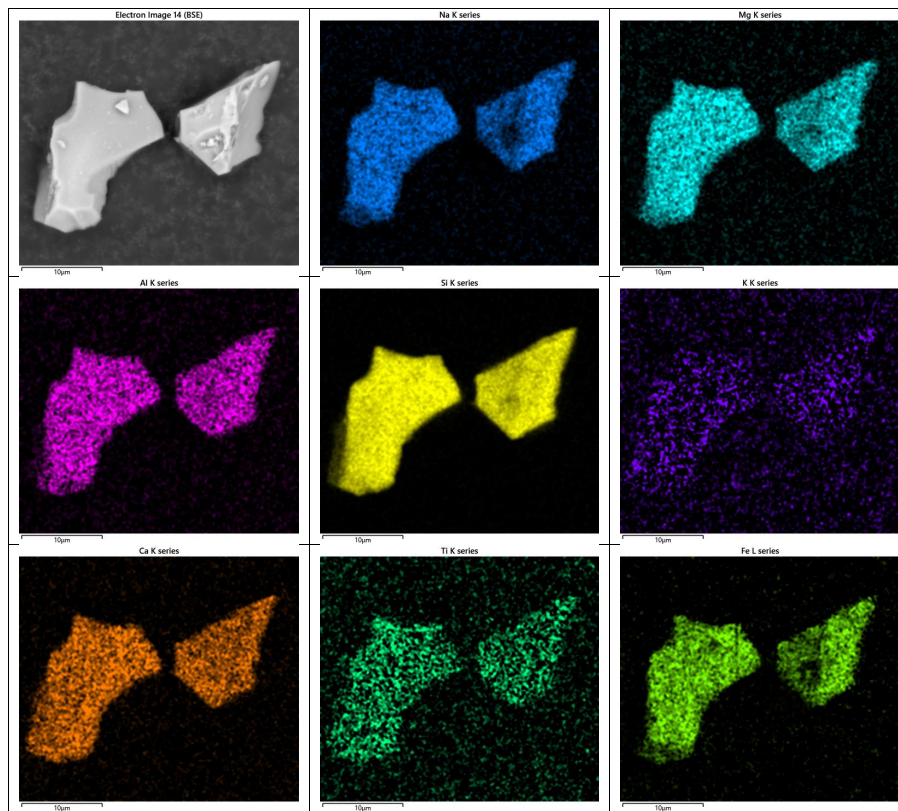
Mg-rich grain



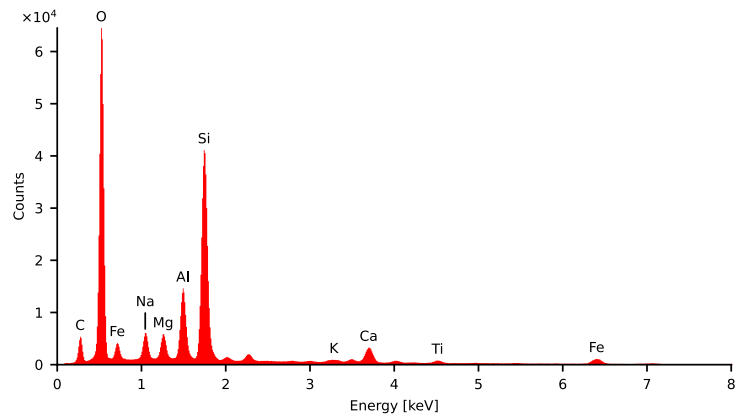
l)



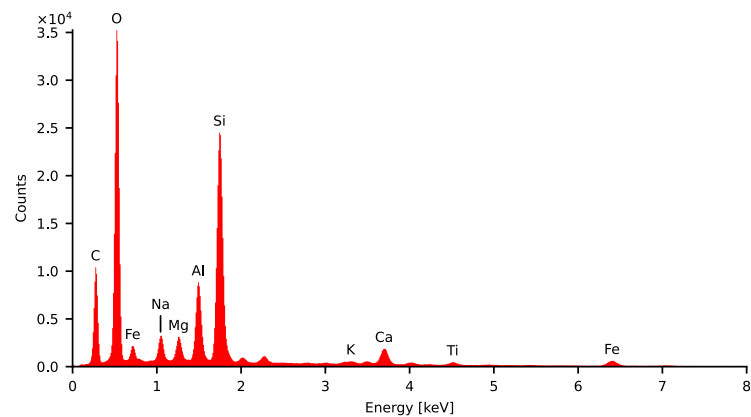
m)



Left particle



Right particle



S10 SEM image of sulfate particle

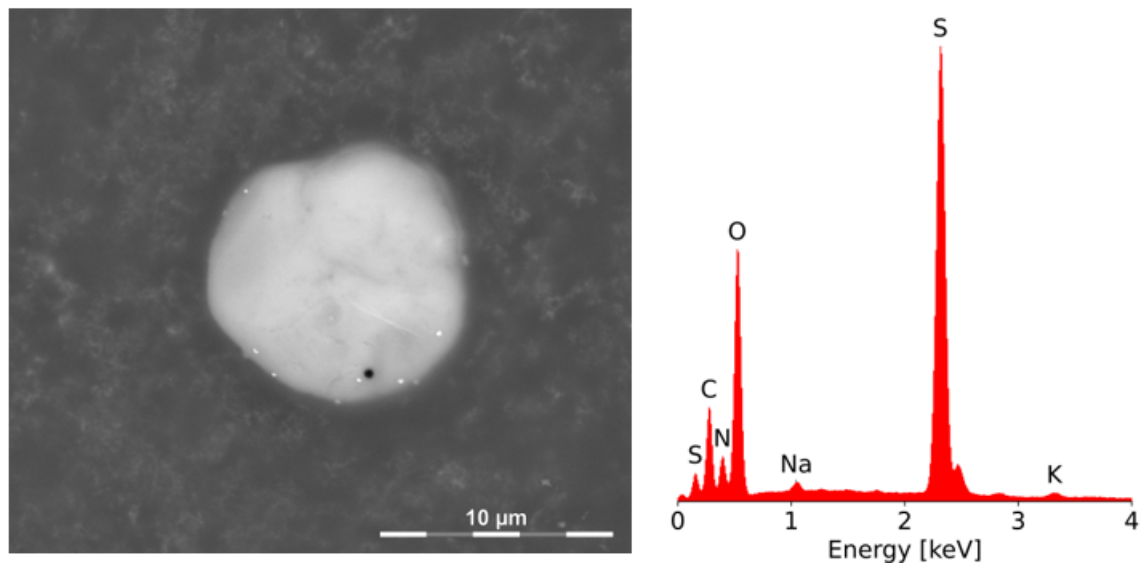
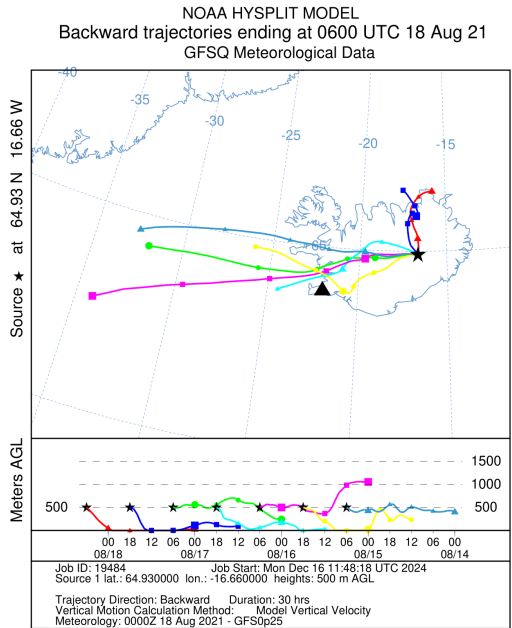


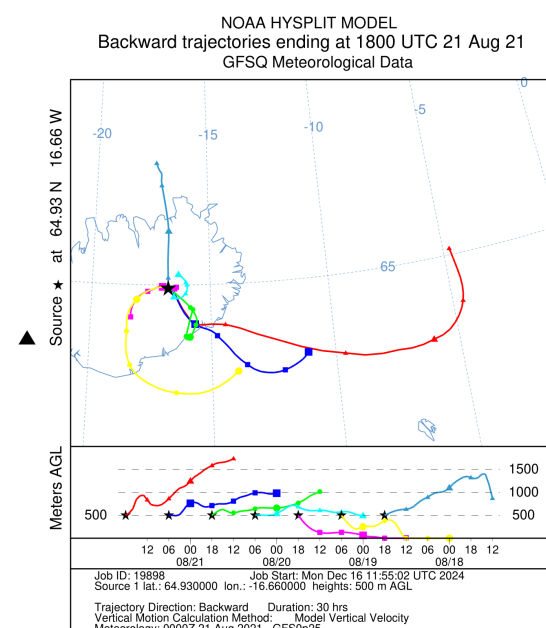
Figure S6. SEM image and its corresponding EDX signal of sulfate particles.

S11 Backward trajectories

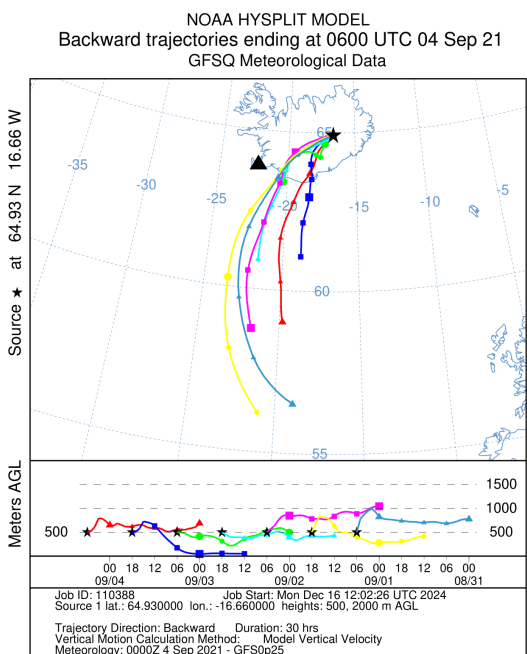
30-h air mass back-trajectories initiated at 500-m above ground level during sulfate episodes for August-September 2021. The calculation parameters are described in the plots themselves (Fig. S7 a-d).



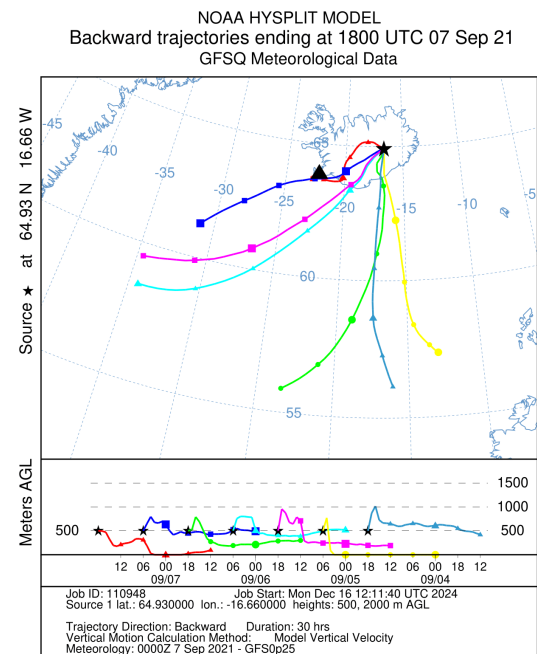
(a)



(b)



(c)



(d)

Figure S7. 30-h air mass back-trajectories for sulfate episodes.